A terminology for 2D grids

Dominique Désérable

INSTITUT NATIONAL DE RECHERCHE EN INFORMATIQUE ET EN AUTOMATIQUE

A terminology for 2D grids

Dominique DESERABLE

N° 2346
Juin 1994

PROGRAMME 1

A terminology for 2D grids

Dominique Désérable*

Programme 1 — Architectures parallèles, bases de données, réseaux et systèmes distribués
Projet API

Rapport de recherche n° 2346 — Juin 1994 — 31 pages

Abstract: Compared with other more sophisticated interconnection topologies, the grid – and its toroidal extension – has several important advantages such as its simplicity of design and its bounded number of communication links for each processing node. Consequently, a lot of work has been done or is still in progress upon grid-based networks. However, the terminology is often imprecise or even non-existent. So, in order to clarify future work in the field of massively parallel architectures, we propose a terminology based on a material borrowed from geometry of tiling and regular figures, regular graph theory or plane crystallography and dealing with the concept of *valence*. The present proposal is restricted to infinite two-dimensional grids.

Key-words: interconnection networks, 2D regular and semiregular grids, 2D crystallography, valence, duality, combinatorial equivalence, Cartesian and hexagonal coordinate systems.

(Résumé : tsvp)

*Institut National des Sciences Appliquées
Campus Universitaire de Beaulieu – 35043 Rennes cedex – France
deserable@irisa.fr

Unité de recherche INRIA Rennes
IRISA, Campus universitaire de Beaulieu, 35042 RENNES Cedex (France)
Téléphone : (33) 99 84 71 00 – Télécopie : (33) 99 84 71 71

Une terminologie pour grilles 2D

Résumé : Comparée à d'autres topologies d'interconnexion plus sophistiquées, la grille – et son extension torique – possède plusieurs avantages importants dont sa simplicité de conception et son nombre borné de liens de communication sur chaque noeud. De ce fait, de nombreux travaux concernant les réseaux en grille ont ete réalisés ou sont toujours en cours. Cependant, la terminologie est souvent imprécise voire inexistante. Aussi, afin de clarifier les travaux futurs dans le domaine des architectures massivement parallèles, on propose une terminologie empruntée a la géométrie des pavages et des figures régulières, la théorie des graphes réguliers ou la crystallographie plane et basée sur la notion de *valence*. Le présent propos est restreint aux grilles bidimensionnelles infinies.

Mots-clé : réseaux d'interconnexion, grilles 2D régulières et semirégulières, crystallographie plane, valence, dualité, équivalence combinatoire, systèmes de coordonnées Cartésien et hexagonal.

Table

1 Introduction

Compared with other more sophisticated interconnection topologies, the grid – and its toroidal extension – has several important advantages such as its simplicity of design and its bounded number of communication links for each processing node. Consequently, a lot of work has been done or is still in progress upon grid-based networks. However, the terminology is often imprecise or even non-existent. Some examples may highlight the lack of accuracy as a guidance : the usual orthogonal grid seems to make up the unique arrangement and thereby is emphatically called "the grid" ; likewise, unsuitable terms such as "square" or "hexagonal" that are misused to define the number of incident links for any node, seem to describe something like the global network boundary and may lead to misunderstanding ; often, a confusion is made between the grid and the underlying tessellation ; and so forth... So, in order to clarify future work in the field of massively parallel architectures, we propose a terminology based on a material borrowed from geometry of tiling and regular figures, regular graph theory or plane crystallography and dealing with the concept of *valence*. A substantial material can be found in Coxeter [1] for a geometrical background, Fejes Toth [2] and Coxeter & Moser [3] for the symmetry of regular figures, Grünbaum & Shephard [4] (and references therein) for a complete and updated theory of tiling, Harary [5] and Biggs [6] respectively for planar and regular graphs and Buerger [7] for crystal geometry. Although those various fields should exceed the scope of the subject, we hope they will provide further developments as a whole. The present proposal is restricted to infinite two-dimensional grids.

Section 2 begins by providing an exhaustive enumeration of all possible *regular* grids through a metrical approach. As a regular graph, a grid is said to be regular of valence p (or p-valent) if each of its vertices has valence p. We recall that there exist only three regular tessellations, tiling the plane with equilateral triangles, squares and regular hexagons. For our concern, centroids of polygons represent the nodes of the grid (the processing elements "PE") while edges represent the communication links. The reasons why our approach is metrical rather than combinatorial are not straightforward. First we can observe that the former way is easy, the latter one is not. But one practical motivation justifying a metrical approach is based on the important notion of *duality* when the choice is governed by the application : besides its general-purpose capability, a p-valent grid may typically be used as a parallel architecture dedicated to the mapping of a 2D scene tessellated into regular p-gons (or "cells") in a divide-and-conquer partitioning strategy (the parallel computer that had been devised by Unger in the fifties is illustrative in this regard [8]). In this typical case, the cell is known as a fundamental or Dirichlet region also called the Voronoi polygon of the tiling. Another more subtle reason is relevant to the problem of how to fill a surface with electronic components in order to arrange an area-efficient layout : it can be observed some metrical analogy with the above problem of how to partition a 2D scene. The definitive reason, however, has a topological nature and will be explained in the sequel.

Section 3 is given up to a review for the following sections. It enumerates the Archimedean and Laves tiling and shows the duality relationship with one another.

In Section 4 we develop a derived class of *semiregular* grids from the observation of a discrepancy between the set of adjacent cells and the set of neighbouring cells in the square and equilateral tessellations. This fact still strengthens the idea of the well-founded character of the above metrical approach since the construction is motived by another application-oriented consideration. Looking at the three regular tessellations and knowing that a p-gonal cell has p adjacent neighbours, we observe that the square has eight neighbours and the triangle has twelve neighbours (whereas the hexagon has exactly six adjacent neighbours). This is a well-known problem for the usual 4-valent grid where a routage of length two is needed to carry out a path on the diagonal. On the contrary, this question is irrelevant for the hexagonal tiling and would give an advantage for the 6-valent grid. We give a systematic way to develop a full class of semiregular grids. A vertex of a new species (a "switch" S) is created and each PE-to-PE edge is removed and replaced by a PE-S-PE path.

As previously mentioned, we next extend, in Section 5, the nature of the proposal from metrical to combinatorial through the concept of *homeomorphism* of tilings. Whereas isometries of the plane are congruent transformations which preserve all distances, homeomorphisms, which can "stretch or compress" the tiling, preserve the valence of vertices and the number of adjacents and neighbours of each tile. They partition the set of all tilings into *types* of topologically equivalent tilings. Finally, it will be shown that topological equivalence and combinatorial equivalence coincide provided that some condition of normality is fulfilled. "Stretch, compress, but don't tear the tiling !" would highlight the notion of normality through an intuitive meaning. Notice that this definition of homeomorphism for tilings has a rather different meaning than for graphs. Now, since homeomorphism preserves adjacency of tiles, then valence and adjacency are preserved for vertices of the corresponding dual grid. Therefore, the grids resulting from a dual transformation of a same topological type are readily isomorphic.

Section 6 illustrates the content of previous sections by showing several existing, or at least realistic configurations of regular and semiregular grids. We display some orthogonal configurations for various types of grids, then emphasize how subvalent grids of the 6-valent grid can be readily embedded onto.

Finally we focus in Section 7 on the problem of labelling the vertices of the grids by some convenient *coordinate systems*. A close problem arose in crystallography, of trying to adjust crystal systems to crystal classes. We explain first the reasons why two systems, namely the Cartesian coordinate system and the hexagonal coordinate system are really of interest. We take care to define the usual Cartesian system, then give a description of the hexagonal system and set up the correspondence with one another. Each of them enables a proper definition of the different types of grids as well as their colorability. The problem of coloring the grid consists here in finding the pertinent relationships between label and colour. A chromatic representation of the grid may help efficient statements for various grid-based problems such as dissemination information. As an example, a 2-coloring would partition the set of nodes of a 4-valent grid into a subset of "senders" and a subset of "receivers" for one step of a global communication process in a half-duplex mode.

2 Regular grids

We first give an enumeration of all possible ways of filling the Euclidean plane with congruent regular polygons, without gaps or overlaps. The arrangement is called a regular *tessellation* (or likewise, a regular *tiling*). For convenience, we use the Schläfli symbol $\{p, q\}$ which denotes a tessellation of p-gons, with q p-gons surrounding each vertex [1]. We choose to define the p-valent grid afterwards from the *dual* tessellation and detail the notion of *Voronoi cell* associated to a vertex of the grid.

2.1 Regular tessellations

The reader can refer to Coxeter [1], Fejes Toth [2] for regular tessellations and Grünbaum & Shephard [4] for this ad hoc version of the following statement. A tiling is *monohedral* if every tile is congruent to one fixed set T. The set T is called the *prototile* of the tiling.

Statement 2.1.1 The only edge-to-edge monohedral tilings by regular polygons are the three regular tilings $\{3,6\}$, $\{4,4\}$ and $\{6,3\}$. They have, as prototiles, an equilateral triangle, a square and a regular hexagon.

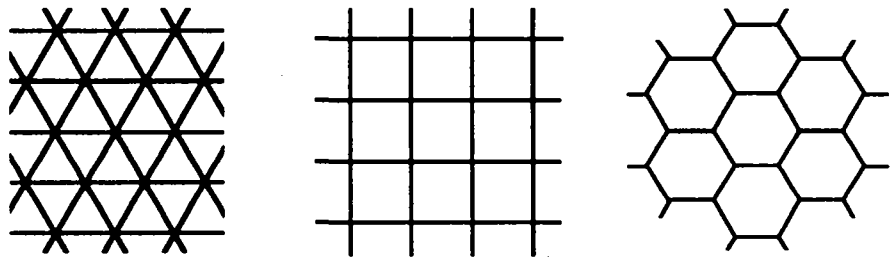

Figure 2.1.1 : The three regular tessellations $\{3,6\}$, $\{4,4\}$ and $\{6,3\}$.

As far as we know, the result would date from Kepler (1619). We give here the elementary proof for a thorough understanding. Equating the angle of a p-gon, namely $(1 - 2/p)\pi$, to the value it must have if q such polygons fit together at a vertex, gives all possible values of p and q, thus :

$$(1 - 2/p)\pi = 2\pi/q$$

giving after transformation :

$$(p - 2)(q - 2) = 4. \qquad (2.1.1)$$

The three possible ways of factorizing 4, namely, $1 \cdot 4$, $2 \cdot 2$, $4 \cdot 1$, yield the three expected tessellations of Figure 2.1.1. Note that p and q must have integer values : fractional values would lead to a set of star tessellations that cannot suit [1]. The above statement underlies a proof of an important result known as the *crystallographic restriction* : the order of a rotation in the symmetry group of a lattice can only be 2 (for a half-turn) or 3, 4, 6. In particular, 5-fold or more than 6-fold rotations are not allowable in infinite lattices [1,7].

2.2 *Dual tessellations and regular p-valent grids*

An elementary definition of *duality* for regular tessellations is borrowed from Coxeter [1] :

Definition 2.2.1 The dual of $\{p,q\}$ is the tessellation whose edges are the perpendicular bisectors of the edges of $\{p,q\}$; the vertices of either are the centres of the faces of the other. Thus the dual of $\{p,q\}$ is $\{q,p\}$ and vice-versa.

Now $\{q,p\}$ is a regular tessellation with q-gons where p is the valence of any vertex. Figure 2.2.1 shows the dual transformation of Figure 2.1.1. Restricting our attention to vertices and edges of the construction and forgetting the indice q for a moment : we have a regular graph of valence p that we shall call a *p-valent grid* in the sequel (refer to the terminology of Biggs in [6] for regular graphs). We observe besides that, according to the crystallographic restriction, the valence *6* is the higher possible valence for a regular planar grid.

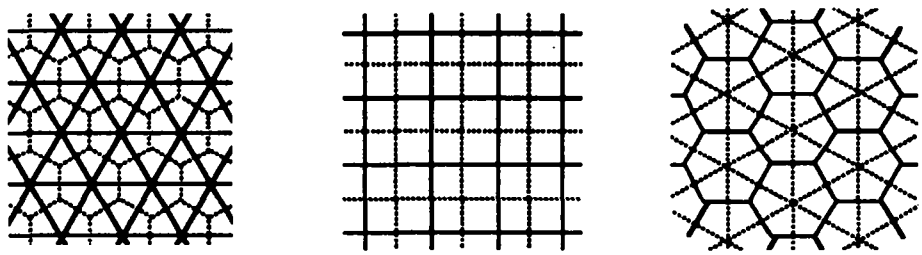

Figure 2.2.1 : The dual tessellations *{6,3}*, *{4,4}* and *{3,6}* of Figure 2.1.1 (in dashed lines)

From now on, the vertices of $\{q,p\}$ will represent the processing elements "PE" (usually called the nodes of the grid) and the edges will represent the PE-to-PE communication links (Figure 2.2.2). Unless it is clear from context, a regular grid should consequently be termed as either *trivalent* or *tetravalent* or *hexavalent* and it is highly hoped that doubtful terms like "hexagonal", "square" or "triangular" will no longer be used. Throughout the paper, a p-valent grid will be generally denoted by the graph ${}^{p}G = ({}^{p}V, {}^{p}E)$ (or shortly $G = (V, E)$ if it is clear from context).

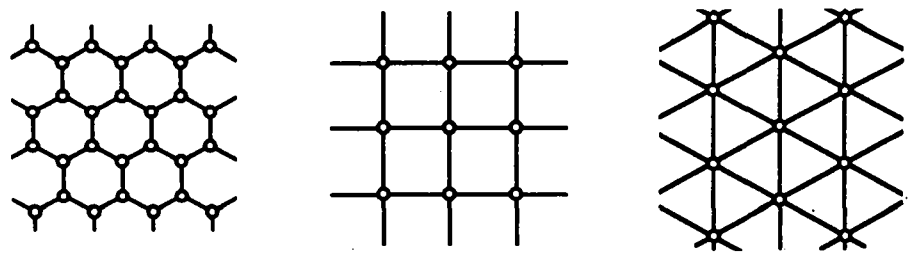

Figure 2.2.2 : The *3*-valent, *4*-valent and *6*-valent regular grids

2.3 Fundamental region and Dirichlet tessellation

A *lattice of points* defines a basic *fundamental region* whose typical feature is the area. On the other hand, a *random set of points* defines a *Dirichlet tessellation* into cells generally known as Voronoi cells. We attempt to unify both notions in our context of regular grids. For the sake of clarity, the notions of fundamental region and Dirichlet tessellation are examined thereafter separately. The underlying idea is to clarify an usual, sometimes confuse processor-cell allocation paradigm.

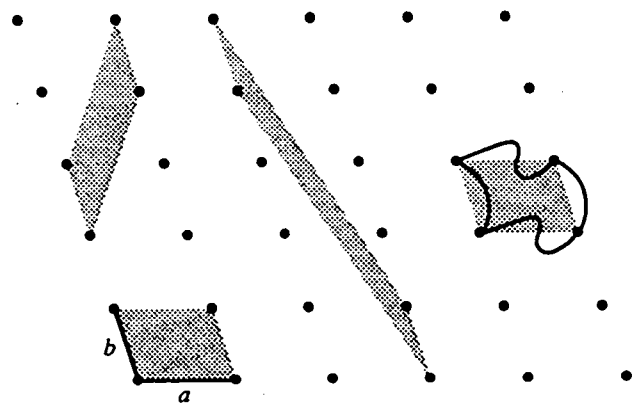

Figure 2.3.1 : A lattice and some fundamental regions

Given two independent vectors $\boldsymbol{a}$ and $\boldsymbol{b}$, a lattice consists of all linear combinations $m\boldsymbol{a} + n\boldsymbol{b}$ where m, $n \in Z$. The typical parallelogram $(\boldsymbol{0}, \boldsymbol{a}, \boldsymbol{b}, \boldsymbol{a} + \boldsymbol{b})$ will define a *fundamental region* for the lattice (Figure 2.3.1). Following the descriptive approach of Coxeter [1], we note that any parallelogram may serve as a fundamental domain whenever its four vertices are lattice points, and no other lattice point lies on its boundary or inside. Such a parallelogram defined by two vectors $\boldsymbol{a}'$ and $\boldsymbol{b}'$ has the typical area of a fundamental region given by the determinant of $[\boldsymbol{a}' \ \boldsymbol{b}']$. But a fundamental region may have any shape provided we keep its area invariant, for example if we turn two opposite sides into congruent curves. Indeed a fundamental region should define a prototile covering the plane without gap or overlap. The most famous application can be found in the art of M. C. Escher who "metamorphosed" basic fundamental domains into various figurative patterns like fishes and birds, angels and demons, beetles, or knights on horseback. Formal definitions of fundamental domains, but which would lead us too far, are given by Grunbaum & Shephard [4] and Fejes Toth [2] from groups of isometries, Coxeter & Moser [3] from generators and Cayley diagrams ; the fundamental region is defined as a *unit* or *primitive cell* in Buerger [7], Fejes Toth [2]. All refer to the 17 two-dimensional *crystallographic groups* usually known in the literature as *wallpaper patterns*.

Among numerous works upon Dirichlet tessellations we follow now a clear description given by Sibson [9] about data analysis because it refers more closely to our - application-oriented - proposal. Given hence a random set of distinct points $S = \{P_1, P_2..., P_N\}$ in the plane, the set :

$$T_n = \{ x : d(x, P_n) < d(x, P_m) \quad \forall m \neq n \}$$

where d is the euclidean distance, defines the "territory" of P_n in the sense that it is the part of the plane nearer to P_n than to the other P_m. T_n is the intersection of open half-planes, the m-th half-plane being bounded by the *perpendicular bisector* of the line $P_n P_m$ and being the half-plane containing P_n. In practice, since the set S is not finite, we have to localize the construction for each P_n inside a topological disk centred in P_n (say a "window") in order to bound the number of half-planes, knowing that any point outside the window will not affect the territory of P_n. This construction achieves a tiling of the plane known as the Dirichlet tessellation defined by S (Figure 2.3.2). A tile T_n defines a polygonal *Dirichlet domain* also known as *Voronoi cells* (or *Thiessen* or sometimes *Wigner-Seitz* cells). The Dirichlet tessellation of a scene into Voronoi cells provides a straightforward spatial divide-and-conquer allocation strategy which is extensively used in 2D application parallel processing.

Remains now to unify the notions of fundamental region (assigned to a lattice) and Voronoi cell (assigned to a random set of points) in our context of regular grids and their dual. We observe in Figure 2.3.3 that a lattice is spanned by the vertices of the *6*-valent and *4*-valent grids. The case of the *3*-valent grid in Figure 2.3.4 is a little more tricky because, instead of forming a lattice, the vertices form two superposed lattices revealed by their bicoloration. So, for the sake of clarity, we shall examine the two situations separately.

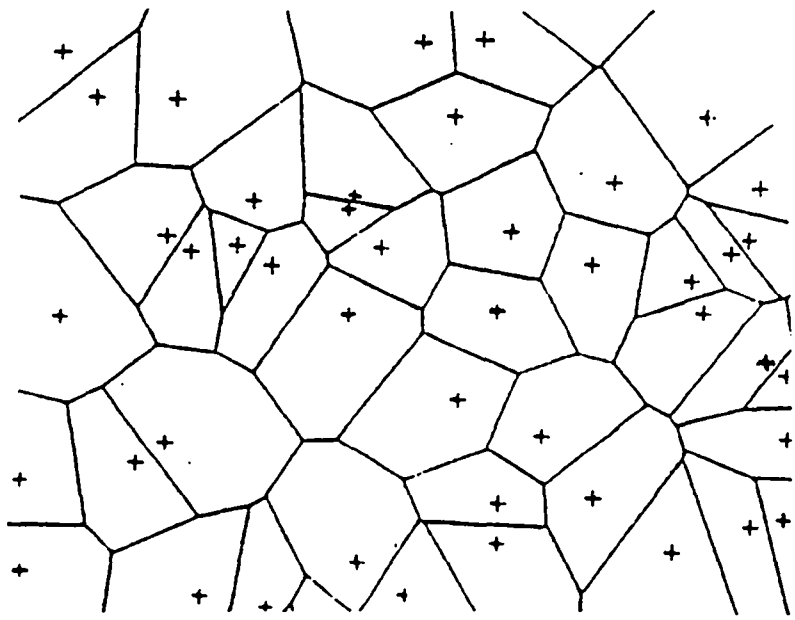

Figure 2.3.2 : Dirichlet tessellation of a random set of points

Proposition 2.3.1 Let ${}^{p}V$ ($p = 4, 6$) be the lattice spanned by the vertices of a p-valent grid and x be any vertex of ${}^{p}V$. The tile $T(x)$ of the dual $\{p, q\}$ whose x is the centroid is the Voronoi cell of x as well as a fundamental region of ${}^{p}V$.

Proof : It is clear that the construction of the Dirichlet tessellation defined on ${}^{p}V$ and of the dual tessellation $\{p,q\}$ with perpendicular bisectors coincide. Hence the tile $T(x)$ of $\{p,q\}$ is the Voronoi cell of x.

In order to show that $T(x)$ is a fundamental region of ${}^{p}V$, we proceed by a dissection of $T(x)$ into labelled subdomains according to Figure 2.3.3. $T(x)$ is composed of p 4-gons whose union is the area of a basic parallelogram P of ${}^{p}V$: subdomains of $T(x)$ and P sharing the same index are pairwise congruent by translation •

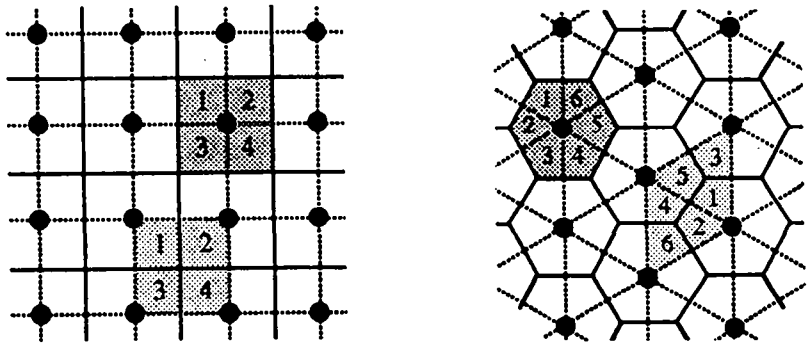

Figure 2.3.3 : Basic fundamental region and Voronoi cell in ${}^{4}G$ and ${}^{6}G$

Proposition 2.3.2 Let ${}^{3}V'$ and ${}^{3}V''$ be the lattices spanned respectively by the black and white vertices of the 3-valent grid and x be any vertex of ${}^{3}V'$ (respectively ${}^{3}V''$). The tile $T(x)$ of the dual $\{3,6\}$ whose x is the centroid is the Voronoi cell of x as well as a half-fundamental region of ${}^{3}V'$ (resp. ${}^{3}V''$).

Proof : As above, the construction of the Dirichlet tessellation defined on ${}^{3}V' \cup {}^{3}V''$ and of the dual tessellation $\{3,6\}$ with perpendicular bisectors coincide. Hence the tile $T(x)$ of $\{3,6\}$ is the Voronoi cell of x.

Observe now in Figure 2.3.4 the parallelogram defined as a fundamental region of ${}^{3}V'$, the parallelogram drawn on ${}^{3}V''$ and the parallelogram formed by the union of two reversed adjacent triangles. It is clear that they can coincide through some adequate translation. Hence $T(x)$ is a half-fundamental region of ${}^{3}V'$ (resp. ${}^{3}V''$) •

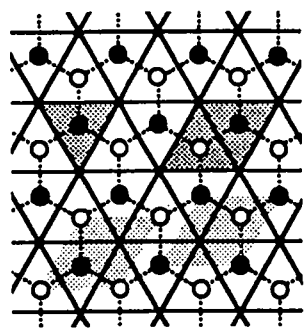

Figure 2.3.4 : Half-fundamental region and Voronoi cell in ${}^{3}G$

3 Archimedean and Laves tilings

This part is given up to a review required for the following sections. It enumerates the *Archimedean* and *Laves* tilings and shows the *duality* relationship with one another. Throughout this section, whose content is borrowed as a whole from Grünbaum & Shephard [4] , the peculiar Schläfli symbol $\{p,q\}$ is ignored but replaced by a more general notation.

3.1 Archimedean tilings

Definition 3.1.1 A vertex is of *type* $n_1.n_2.\ ...\ .n_r$ if it is surrounded by an n_1 -gon, an n_2 -gon, ... and an n_r -gon, all regular, in cyclic order. A lexicographical notation will be chosen in order to have a unique symbol for each type of vertex.
A tiling is said to be of *type* $(n_1.n_2.\ ...\ .n_r)$ if each vertex have the same type $n_1.n_2.\ ...\ .n_r$. Superscripts will be used to abbreviate the notation when possible.

Theorem 3.1.1 There exist 11 distinct edge-to-edge tilings by regular polygons such that all vertices are of the same type. These are (3^6), $(3^4.6)$, $(3^3.4^2)$, $(3^2.4.3.4)$, $(3.4.6.4)$, $(3.6.3.6)$, (3.12^2), (4^4), $(4.6.12)$, (4.8^2) and (6^3).

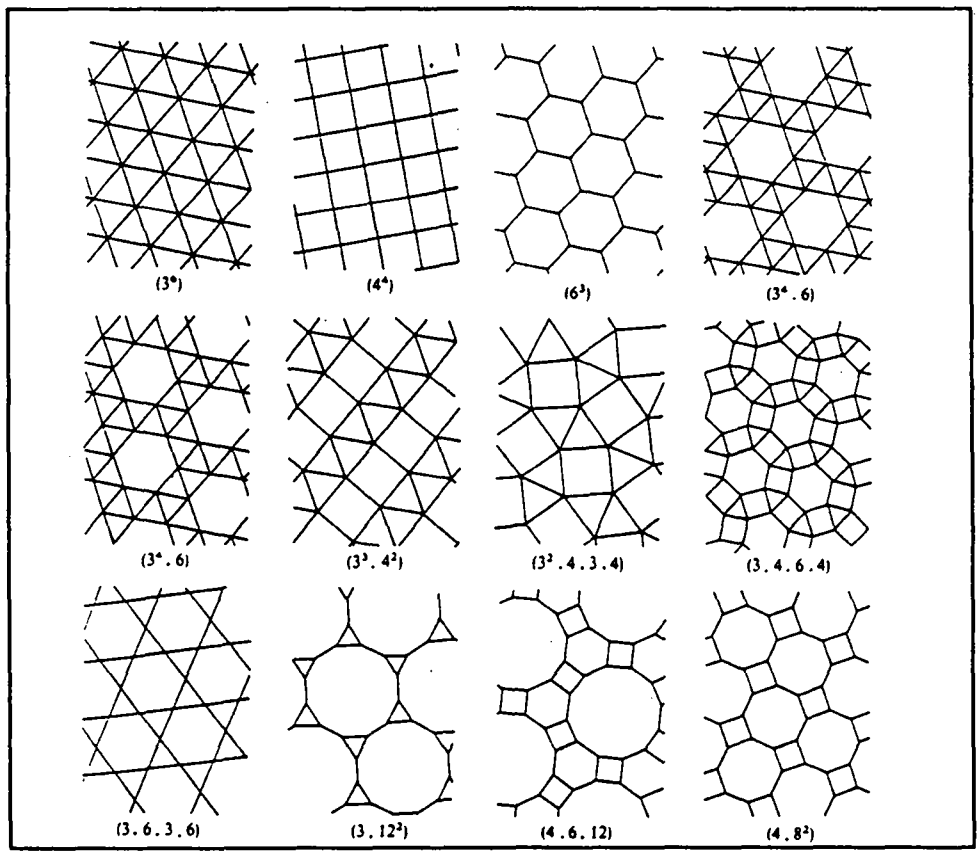

Figure 3.1.1 : The eleven Archimedean tilings

Those eleven tilings are usually called *Archimedean* or sometimes *uniform* tilings. We give some hints for understanding, the reader is referred to Grünbaum & Shephard [4] for the ultimate proof. Recall that the angle of a regular n-gon has the value $(n\text{-}2)\pi/n$. If r polygons can fit around a vertex then :

$$(n_1 - 2)/n_1 + \ldots + (n_r - 2)/n_r = 2. \qquad (3.1.1)$$

It can be checked that only 17 choices of $n_1.n_2.\ldots.n_r$ satisfy the equation. Reversal or cyclic orders of the sequence are not considered as distinct. Now some sequences can lead to other allowed permutations giving exactly 21 types of vertices altogether. However all of those 21 types do not suit for tiling the plane. A thorough elimination of the unsuitable types leads to the 11 types of Figure 3.1.1. Observe that the three regular tilings denoted here (3^6), (4^4) and (6^3) are the only monohedral tilings. Note besides that there are two tilings of type $(3^4.6)$ that can coincide only by reflection : they are called "enantiomorphic" forms (or mirror images).

3.2 Laves tilings

Definition 3.2.1 A vertex of valence v is called regular if the angle between each consecutive pair of edges is $2\pi/v$. A monohedral tiling with tiles whose vertices have valences $v_1.v_2.\ldots.v_r$ will be denoted by $[v_1.v_2.\ldots.v_r]$ with superscripts used to abbreviate the notation when possible.

Theorem 3.2.1 There exist 11 monohedral tilings with regular vertices. These are $[3^6]$, $[3^4.6]$, $[3^3.4^2]$, $[3^2.4.3.4]$, $[3.4.6.4]$, $[3.6.3.6]$, $[3.12^2]$, $[4^4]$, $[4.6.12]$, $[4.8^2]$ and $[6^3]$.

Those eleven tilings are usually called *Laves* tilings (after the crystallographer Fritz Laves). Since we consider monohedral tilings, assume the prototile as an r-gon with vertices of valence $v_1.v_2.\ldots.v_r$. Recall that the sum of the angles of a r-gon is $(r\text{-}2)\pi$, then :

$$2\pi/v_1 + \ldots + 2\pi/v_r = (r\text{-}2)\pi.$$

equation which can be rearranged as equation (3.1.1) with :

$$(v_1 - 2)/v_1 + \ldots + (v_r - 2)/v_r = 2. \qquad (3.2.1)$$

In the same way, we obtain 17 solutions leading to 21 cases $v_1.v_2.\ldots.v_r$ taken cyclically around a tile. A simple elimination of the unsuitable cases leads to the 11 tilings of Figure 3.2.1. Observe that $[3^6]$, $[4^4]$ and $[6^3]$ are the only Laves tilings by regular polygons. Observe besides that $[3^4.6]$ occurs in two enantiomorphic forms. We should also be aware of the following fact : let us examine the Laves tiling $[4^4]$ in particular ; if we "stretch" the tiling in one direction we obtain a (topologically equivalent) tiling with a rectangular prototile (see Section 5 for detail) that still satisfies Theorem 3.2.1, in other words it remains a monohedral tiling with regular vertices, thus there exist an infinite number of such tilings depending on a real-valued parameter. We finally choose to fix the prototile as a square prototile. A similar remark concerns the tilings $[3^6]$ and $[3^3.4^2]$.

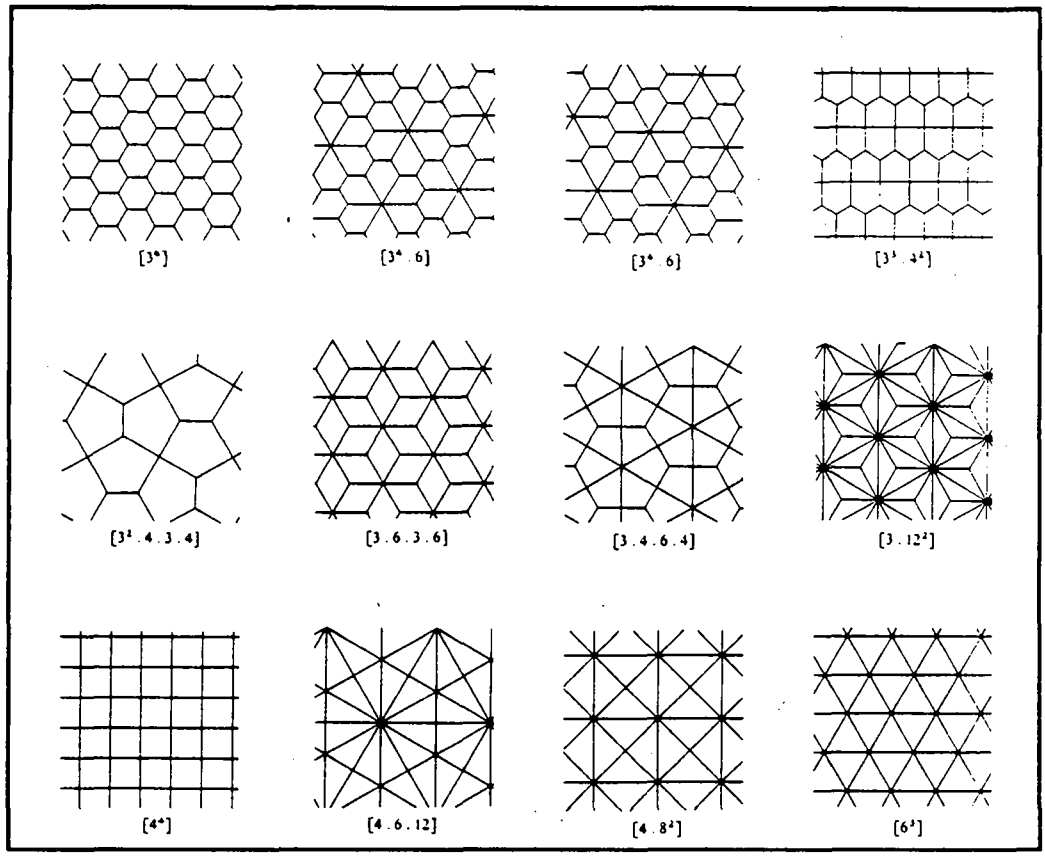

Figure 3.2.1 : The eleven Laves tilings

3.3 Duality

Definition 3.3.1 Two tilings τ and τ^* are said to be *dual* to each other if there exists a one-to-one *inclusion-reversing* correspondence φ from the set of elements of τ onto the set of elements of τ^*. In other words, whenever e_1 and e_2 are elements of τ, then $\varphi(e_1)$ includes $\varphi(e_2)$ iff e_2 includes e_1.

Theorem 3.3.1 Let τ be any Archimedean tiling $(v_1.v_2.\ \ldots\ .v_r)$ and τ^* the corresponding Laves tiling $[v_1.v_2.\ \ldots\ .v_r]$: τ and τ^* are dual to each other.

Clearly we can set up a one-to-one correspondence between the tiles, edges and vertices of τ onto the vertices, edges and tiles of τ^* in such a way that inclusion is reversed : if, for example, a given tile contains a certain vertex in τ, then in τ^* the corresponding vertex is contained in the corresponding tile. The reader may check the duality by superimposing on any tiling τ of Figure 3.1.1 a dual tiling τ^* in such a way that edges of τ and edges of τ^* intersect at *right* angles, then by processing the reverse construction $\tau^* \rightarrow \tau$ on Figure 3.2.1 afterwards.

Notice that Definition 2.2.1 in Section 2 was a particular case for regular polygons since the dual construction of $\{q,p\}$ from $\{p,q\}$ with perpendicular *bisectors* was more restrictive.

4 Semiregular grids

4.1 Adjacency in regular tessellations

The following development is motived by another application-oriented consideration. Figure 4.1.1 is representative of a scene partitioned into square cells whose control is assigned to a network of processing nodes. While it is clearly observed that the central node has four neighbours, its corresponding cell is nevertheless surrounded by a neighbourhood of eight cells : four of them are adjacent whereas the other four are diagonally arranged, regarding their position with respect to the central cell. Passing information "on the diagonal" will thus require a *routage* of length 2 cutting through an intermediate node. It is a well-known cumbersome problem encountered furthermore in a large set of applications such as image processing [10], matrix computation, partial differential equations and so on. We attempt to formalize the problem in the following.

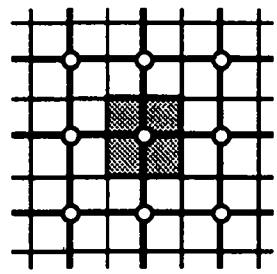

Figure 4.1.1 : A partitioned scene with its assigned network of processors

Proposition 4.1.1 A tile in the $\{p,q\}$ tessellation has $2q$ neighbours and $2q-p$ of them are non-adjacent neighbours.

Proof A tile of $\{p,q\}$ has p vertices (say, p "corners") and $(q-1)$ neighbouring tiles regarding each corner. The product contributes twice on every edge of the p-gon, the count $p(q-1)-p = p(q-2)$ gives hence the number of neighbours. But $p(q-2) = 2q$ from relation 2.1.1. Then the count $2q-p$ gives the number of non-adjacent neighbours, since p are adjacent •

$\{p,q\}$	$\{3,6\}$	$\{4,4\}$	$\{6,3\}$
$v = 2q$	12	8	6
$\alpha = p$	3	4	6
$v-\alpha$	9	4	0

Table 4.1.1 : Number of neighbours (v), adjacent (α) and non-adjacent ($v-\alpha$), related to a tile of $\{p,q\}$

The result of Proposition above is displayed in Table 4.1.1. We first observe that the terms "adjacent" and "neighbour" are synonymous for the hexagonal tessellation $\{6,3\}$, that makes an advantage for the 6-valent grid. Incidentally, the square cell of $\{4,4\}$ has four neighbours at distance 1 and four at distance $\sqrt{2}$, regarding the usual distance between centroids and choosing a unit distance for a pair of centroids of adjacent cells ; likewise, the triangular cell of $\{3,6\}$ has three neighbours at distance 1, six at distance $\sqrt{3}$ and three at distance 2 (see Figure 4.1.2).

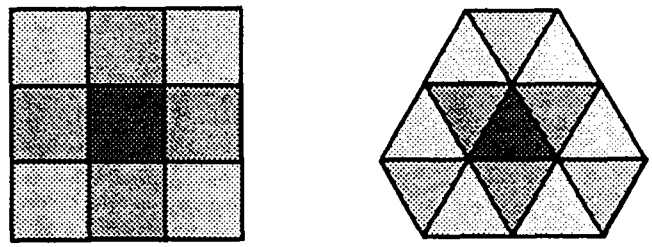

Figure 4.1.2 : The neighbourhood of a tile of $\{4,4\}$ and $\{3,6\}$

4.2 From regular to semiregular grids

The configuration of $\{4,4\}$ (resp. $\{3,6\}$) tells now in creating a regular 8-valent (resp. 12-valent) grid. If a condition of planarity is required besides, as it is often the case for VLSI layout requirements, that condition is unfortunately not satisfied for those grids. This fact is attested in the previous section and highlighted by observing the Archimedean tilings $(4.8.8)$ and $(3.12.12)$ in Figure 3.1.1 : tiling the plane with regular 8-gons or 12-gons without gaps cannot hold.

In addition to the set of processing elements (the "PE-nodes"), we create a new species of node, namely a *switch* (or "S-node"), whose role is to turn any elementary PE-to-PE path of an idealized 8-valent or 12-valent interconnection structure into a mixed PE-S-PE path in order to restore both planarity and symmetry (regarding distance between neighbours). Such a definition of switch was encountered in particular in the polymorphic CHiP architecture of Snyder [11] ; while our purpose does differ a bit, our switch is functionally the same. The way to develop a full class of *semiregular* grids is as follows. Although the matter is irrelevant for the 6-valent grid, nevertheless we generalize the problem for any regular grid through a systematic approach.

Proposition 4.2.1 From any regular p-valent grid there exists a derived semiregular grid induced by the Laves tiling $[p.q.p.q]$ where $q=2p/(p-2)$. Any PE-node is p-valent and connected with p S-nodes whereas any S-node is q-valent and connected with q PE-nodes.

Proof Let us consider a p-valent grid that defines the $\{q,p\}$ tessellation of Section 2.2 together with its dual tessellation $\{p,q\}$. Recall that one PE-node is assigned to any vertex of $\{q,p\}$. Let us assign one S-node to any vertex of $\{p,q\}$ (in other words, a switch is created at the centroid of any tile of $\{q,p\}$) and connect the switch to each corner of its corresponding tile. From the 3-valent, 4-valent

and 6-valent grids, we obtain respectively the Laves tilings [*6.6.6*], [*4.8.8*] and [*3.12.12*] (our index in boldface stands here for a switch) : refer to the previous section where the whole set of Laves tilings is exhibited and compare with their dual Archimedean (*6.6.6*), (*4.8.8*) and (*3.12.12*). Removing all PE-to-PE connections that should be no longer used, we obtain finally the three semiregular configurations [*3.6.3.6*], *[4.4.4.4]* and [*6.3.6.3*] of Figure 4.2.1. Since the two first indices give the Schläfli symbol of the associated tiling in Proposition 4.1.1, thereby $q=2p/(p-2)$ from relation 2.1.1 •

We suggest to denote a semiregular grid by the bipartite graph ${}^{(p,q)}G = ({}^{P}V \cup {}^{q}V, {}^{(p,q)}E)$ where ${}^{P}V$ stands for the set of PE-nodes, ${}^{q}V$ the set of switches, whereas ${}^{(p,q)}E$ stands for the set of edges incident to ${}^{P}V$ and ${}^{q}V$.

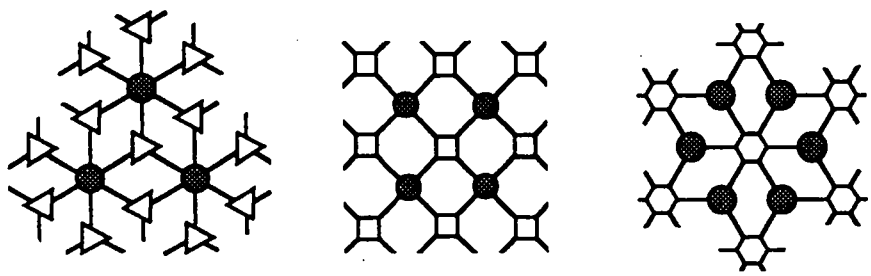

Figure 4.2.1 : The semiregular grids ${}^{(3,6)}G$, ${}^{(4,4)}G$ and ${}^{(6,3)}G$

Corollary 4.2.1 Any PE-node of a semiregular grid ${}^{(p,q)}G$ can access $v=2q$ PE-nodes along paths of length 2 cutting through one S-node. There exist one redundant path for $\alpha=p$ of them and one unique path for the $(v-\alpha)$ others •

The result of this Corollary readily meets the requirement underlying Proposition 4.1.1. We shall henceforth use the term "semiregular" for any grid of that kind.

5 Types of grids and isomorphism

Two grids are said to be of the same *type* if they are *isomorphic*. The purpose of this section is to show that there exist exactly three types of *regular* and three types of *semiregular* grids. It is indeed an established fact that two graphs are isomorphic if there exist a one-to-one correspondence between their vertices which preserves adjacency [5]. However, since an *enumeration* of all possible cases must be undertaken, some more material is required here. The development is based on the topology of tilings. It can be shown that any of the eleven Archimedean tilings defines an equivalence class of topologically vertex-transitive tilings and, on the other hand, any of the eleven Laves tilings defines a class of topologically tile-transitive tilings. Our regular and semiregular types are therefore obtained as specific cases. The material hereto is again borrowed from Grünbaum & Shephard [4] and concerns the topology of "well-behaved" tilings. The content of this section may seem unduly heavy to show an "obvious" fact as in Figure 5.1.1, but it will enable us to assert that our enumeration in the field of regular and semiregular grids is *exhaustive*.

5.1 Combinatorial and topological types of tilings

Definition 5.1.1 Two tilings τ and τ' are said to be *combinatorially equivalent* (or *isomorphic*) if there exists a one-to-one *inclusion-preserving* correspondence ψ from the set of elements of τ onto the set of elements of τ'.

In other words, whenever e_1 and e_2 are elements of τ then $\psi(e_1)$ includes $\psi(e_2)$ iff e_1 includes e_2.

For example, if v is any n-valent vertex of τ then $\psi(v)$ will be an n-valent vertex of the isomorphic tiling τ'. If a tile T of τ has n adjacents then the corresponding tile $\psi(T)$ of τ' will have n adjacents.

Combinatorial equivalence is readily an equivalence relation.

Definition 5.1.2 A mapping $\phi : E_2 \rightarrow E_2$ of the Euclidean plane into itself is called a *homeomorphism* if it is one-to-one and bicontinuous (i.e. ϕ and ϕ^{-1} are continuous).

Two tilings are said to be homeomorphic or *topologically equivalent* if there exist a homeomorphism which maps one onto the other.

It should be clear that topological equivalence is an equivalence relation which partitions the set of all tilings into *topological types*. Figure 5.1.1 shows an example of three homeomorphic tilings. Transforming the the $\{6,3\}$ tessellation (b) into the stretched honeycomb (a) or into the brickwork (c) can be represented in some coordinate system using equations of functions. Such functions will in any case be one-to-one and bicontinuous. Observe that valence and adjacency are preserved during the transformation.

We introduce now a condition of *normality* in order to restrict ourselves to a class of "well-behaved" tilings. That means that a tile in a normal tiling should be neither too thin nor too large...

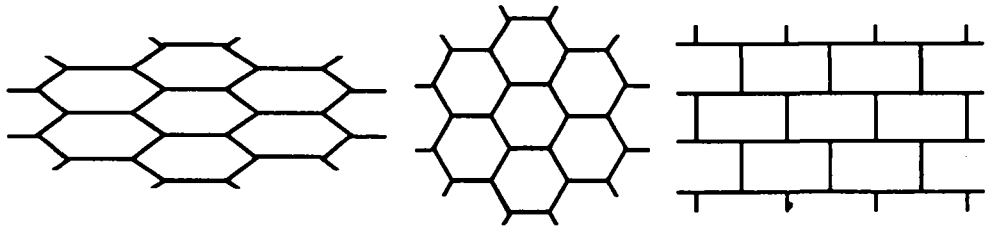

Figure 5.1.1 : Homeomorphic tilings

Definition 5.1.3 A tiling is *normal* if : (i) every tile is a topological disk : in other words, every tile is the image of a circular disk under a homeomorphism ; (ii) the intersection of every two tiles is a connected set : the intersection is either empty or does not consist of two or more disjoint parts ; (iii) the tiles are uniformly bounded : every tile contains some circular disk of radius r and is contained in some circular disk of radius R.

The following statements are a consequence of normality and will turn out to be useful for the sequel.

Statement 5.1.1 For normal tilings the concept of topological equivalence and combinatorial equivalence coincide.

Statement 5.1.2 For every normal tiling τ there exists a normal tiling τ^* which is dual to τ.

5.2 Enumeration of homeogonal and homogeneous types of tilings

Two important statements result from Euler's formula for planar maps (see also Harary [5]). The subjacent reason is that, if V and E stand for the average number of vertices and edges per tile of a (infinite) tiling then $V - E + 1 = 0$ and that Euler's formula can be applied here only because the tiling is *normal*.

Statement 5.2.1 If every vertex of a normal tiling has valence j and is incident with tiles which have k_1, k_2 ... k_j adjacents, then :

$$(k_1 - 2)/k_1 + \ldots + (k_j - 2)/k_j = 2. \qquad (5.2.1)$$

Apply Euler's formula with $V = \sum_{i=1,j} 1/k_i$ and $E = j/2$.

Statement 5.2.2 If every tile of a normal tiling has k vertices and these vertices have valences j_1, j_2 ... j_k then :

$$(j_1 - 2)/j_1 + \ldots + (j_j - 2)/j_k = 2. \qquad (5.2.2)$$

In a similar way, apply Euler's formula with $V = \sum_{i=1,k} 1/j_i$ and $E = k/2$.

Equations of the above statements are the same as equations (3.1.1) and (3.2.1) about Archimedean and

Laves tilings ! The relative weakness of the condition of *normality* required here for (5.2.1) and (5.2.2) is quite noteworthy compared with the strong metric conditions of regular polygons and regular valences : whereas the derivation of equations (3.1.1) and (3.2.1) was *metrical* in that they depended on calculation of angles, equations (5.2.1) and (5.2.2) are of a *combinatorial* (or a topological) nature in that their derivation depend *only* on valences and number of adjacents (Grünbaum & Shephard note yet that the assumption of normality can be regarded as a "hidden" metric condition).

Definition 5.2.1 A normal tiling τ is *homeogonal* (or topologically vertex-transitive) if for any two vertices V_1, V_2 there exists a homeomorphism that maps τ onto itself and V_1 onto V_2. A vertex of τ is of *type* $k_1.k_2.\ \ldots\ .k_j$ if it is surrounded by j tiles having respectively $k_1, k_2, \ldots, k_j$ vertices (in a suitable cyclic order).
The tiling τ is said to be *homeogonal of type* $(k_1.k_2.\ \ldots\ .k_j)$ if any vertex has this same type.

Theorem 5.2.1 If a tiling is homeogonal then it has one of the 11 types (3^6), $(3^4.6)$, $(3^3.4^2)$, $(3^2.4.3.4)$, $(3.4.6.4)$, $(3.6.3.6)$, (3.12^2), (4^4), $(4.6.12)$, (4.8^2) and (6^3). Furthermore, the eleven Archimedean tilings of Figure 3.1.1 define a set of representatives for each (normal) homeogonal type.

The proof follows from Statement 5.2.1 and Theorem 3.1.1.

Definition 5.2.2 A normal tiling τ is *homeohedral* (or topologically tile-transitive) if for any two tiles T_1, T_2 there exists a homeomorphism that maps τ onto itself and T_1 onto T_2. A tile of τ is of *valence-type* $j_1.j_2.\ \ldots\ .j_k$ if it has k vertices with valence $j_1, j_2, \ldots, j_k$ vertices (in a suitable cyclic order).
The tiling τ is said to be *homogeneous of type* $(j_1.j_2.\ \ldots\ .j_k)$ if any tile has this same valence-type. Any homeohedral tiling is readily homogeneous.

Theorem 5.2.2 If a tiling is homeohedral then it has one of the 11 types $[3^6]$, $[3^4.6]$, $[3^3.4^2]$, $[3^2.4.3.4]$, $[3.4.6.4]$, $[3.6.3.6]$, $[3.12^2]$, $[4^4]$, $[4.6.12]$, $[4.8^2]$ and $[6^3]$. Furthermore, the eleven Laves tilings of Figure 3.2.1 define a set of representatives for each (normal) homeohedral type.

The proof follows from Statement 5.2.2 and Theorem 3.2.1.

We finally close this section by tying homeogonal and homeohedral tilings through the notion of duality. Refer to Definition 3.3.1 and Statement 5.1.2 for elements of understanding.

Theorem 5.2.3 Let τ and τ^* be two normal, dual tilings. Then τ is homeogonal iff τ^* is homeohedral.

As it will be illustrated through some typical examples in the following section, we can henceforth assert that any configuration of p-valent grid, whether it is orthogonal, skewed, diamond-shaped and so forth..., belongs to one of the three representative types ${}^3G$, ${}^4G$ or ${}^6G$. Any semiregular grid will be of type ${}^{(3.6)}G$, ${}^{(4.4)}G$ or ${}^{(6.3)}G$. Section 7 will assign coordinates to the set of vertices for usual cases and will show how an isomorphism of grids can be expressed thereby.

6 Typical configurations

We illustrate the content of previous sections by showing several realistic configurations of regular and semiregular grids. Some of them exist while some others could do. Although the classification into topological types allows any atypical arrangement, metric constraints must obviously be taken into account for practical use, whenever the simple requirement of regularity is needed. Angles of interest are induced by the symmetries of regular tilings. This fact is related to the problem of choosing some convenient coordinate system examined in the following section. Two essential categories of arrangement, namely "orthogonal" with angles in $\{k\pi/4 \ ; \ k=0,\ldots,4\}$ and "hexagonal" with angles in $\{k\pi/6 \ ; \ k=0,\ldots,6\}$ are highlighted below through relevant examples.

6.1 Some orthogonal configurations

Figure 6.1.1(a) shows the usual, orthogonal configuration of the *4*-valent grid, the ancient [8, 12] and up-to-date [13] archetype of parallel architectures for supercomputing as well as countless species dedicated to applications such as image processing.

Figure 6.1.1(b) shows an usual, orthogonal configuration of the *6*-valent grid, more specially known in systolic arrays [14, 15]. It can be viewed as the usual grid of (a) on which a diagonal direction of links has been added.

Figure 6.1.2 shows how a *3*-valent grid can be embedded onto *4*-valent as well as *6*-valent orthogonal grids. The representation in (a) is also encountered as a *3*-spanner[1] of the *4*-valent grid [16, 17]. In (b) grey nodes are unused or "disconnected".

Figure 6.1.3 shows a type of $^{(3,6)}G$ semiregular configuration. The role of the *6*-valent switch and of the *3*-valent processing node can be reversed to produce a grid $^{(6,3)}G$. Compare with the corresponding configuration of Figure 4.2.1. As far as we know, configuration 6.1.2(b) and 6.1.3 would have been seldom or never seen.

Figure 6.1.4 shows a semiregular configuration $^{(4,4)}G$ supporting recent SIMD[2] architectures such as BLITZEN [18] and X-Net MasPar MP-1 [19]. They are well suited for image processing, matrix computation and, more generally, for dealing with square (or rectangular) tessellated 2D scenes.

[1] A t-spanner of a network is a subnetwork in which every two nodes that were connected by an edge in the original network are connected by a path of at most t edges in the subnetwork.

[2] Single Instruction Multiple Data

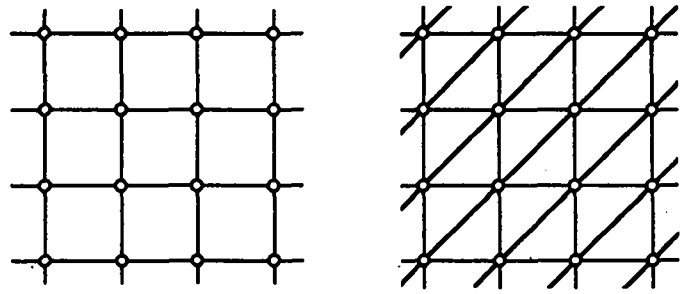

(a) (b)

Figure 6.1.1 : Orthogonal configuration : - (a) of ${}^4G$ - (b) of ${}^6G$

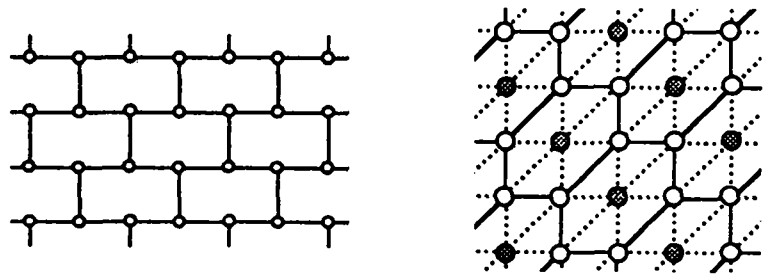

(a) (b)

Figure 6.1.2 : Embedding a 3-valent grid onto : - (a) an orthogonal ${}^4G$ - (b) an orthogonal ${}^6G$

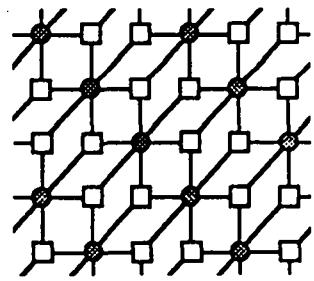

Figure 6.1.3 : Orthogonal configuration of ${}^{(3,6)}G$

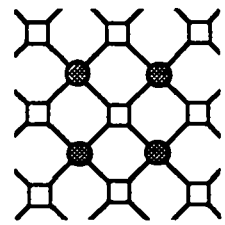

Figure 6.1.4 : The semiregular grid ${}^{(4,4)}G$

6.2 Subvalent grids of the 6-valent grid

Pertinent "hexagonal" configurations may be presented through a unified way as subvalent grids of the isotropic *6*-valent grid. Very simple embedding schemes can be readily carried out for *4*-valent as well as *3*-valent grids, owing to the highest symmetry whose the hexavalent grid is provided. This feature should be regarded as an additional powerful capability turning again out to the advantage of the *6*-valent grid. The following is just an introductory development and will be pursued elsewhere.

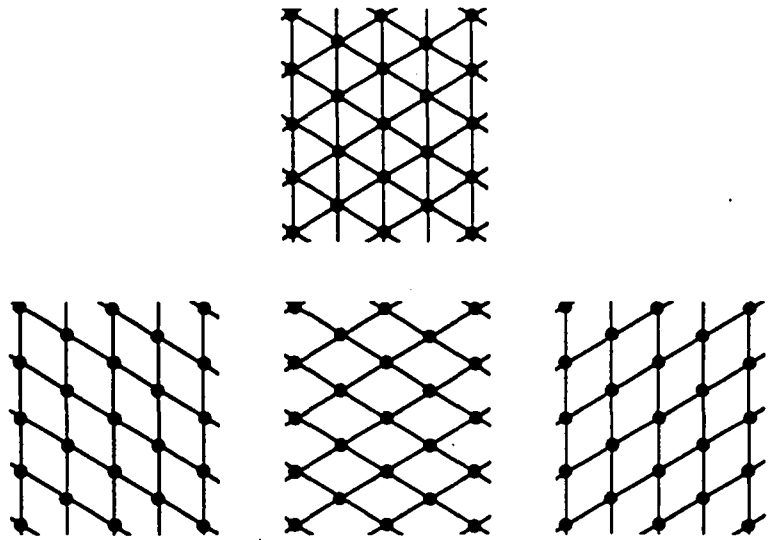

Figure 6.2.1 : Embedding *4*-valent grids onto the *6*-valent grid

Figure 6.2.1 shows three skewed configurations of *4*-valent spanning subgrids ${}^4G_k$ ($k=1,2,3$) embedded onto ${}^6G$. Each subgrid is merely obtained by removing one direction of edges. Incidentally, note that whatever skewed configuration we choose, each subgrid displays a diamond-shaped basic fundamental region of its own, while the Voronoi cell of a given node (which acts thereby as another fundamental region) remains invariant : as a fixed, regular hexagon, it is coincident with the corresponding Voronoi cell in ${}^6G$ (see Figure 6.2.2).

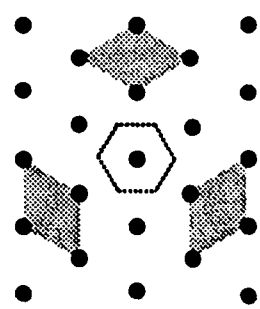

Figure 6.2.2 : A common Voronoi cell and three proper fundamental regions

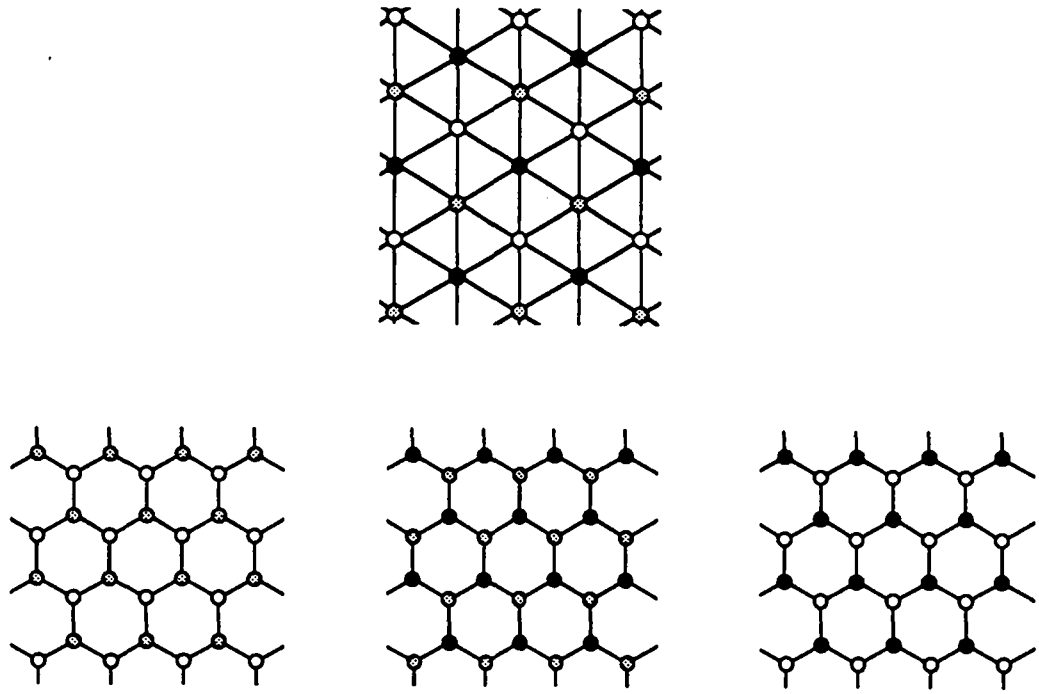

Figure 6.2.3 : Embedding 3-valent grids onto ${}^6G$

Figure 6.2.3 shows three configurations of 3-valent subgrids ${}^3G_k$ ($k=0, 1, 2$) embedded onto ${}^6G$. For convenience, we use the fact that ${}^6G$ is 3-chromatic in order to partition the set of vertices into three color classes ${}^6V = V_0 \cup V_1 \cup V_2$ (refer to the coloring problem in Harary [5] or see Section 7 for details). The removal of any subset V_k leads to a 2-chromatic trivalent induced subgrid since any vertex of ${}^6V - V_k$ is incident to three vertices of V_k. Therefore, ${}^6G$ admits three *edge-disjoint* 3-valent subgrids ${}^3G_k$ whose union is ${}^6G$.

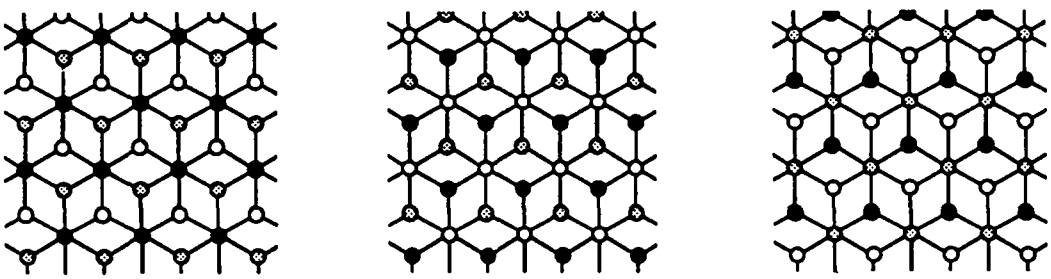

Figure 6.2.4 : Embedding semiregular grids ${}^{(3,6)}G$ onto ${}^6G$

Finally, the union of any pair ${}^3G_{k'} \cup {}^3G_{k''}$ ($k' \neq k''$) gives one among three possible configurations of semiregular grids ${}^{(3,6)}G_k$ as bipartite graphs shown in Figure 6.2.4. We do not regard here the species of any vertex, whether it stands for a switch or a processing node. Such a configuration is readily a

spanning subgrid of ${}^6G$ and, on the other hand, seeing that $V_k = {}^6V - (V_{k'} \cup V_{k''})$, the relevant subgrid is "k-dominant" in the sense that any vertex of V_k is 6-valent whereas any vertex of ${}^6V - V_k$ is 3-valent.

As far as we know, such subvalent arrangements have not been encountered in the literature. Concerning actual hexavalent architectures, except within the systolic field through orthogonal layouts, they are rather unusual. Let us make mention of the ancient ILLIAC III project [20] (mixing both tetravalent and hexavalent types) and the Golay's machine [21] dedicated to pattern recognition ; the FAIM-1 project [22] for artificial intelligence, giving subsequently rise to the HARTS project [23] for real-time systems... The author is currently working on a general-purpose project thereupon.

7 Coordinate systems

We focus finally on the problem of labelling the vertices of the grids by some convenient *coordinate systems*. We explain first the reasons why two systems, namely the Cartesian coordinate system and the hexagonal coordinate system, often denoted "CCS" and "HCS" in the sequel, are really of interest. We take care to define the usual CCS then give a description of the HCS and set up the correspondence with one another. Each of them enables a proper definition of the different types of grids as well as their colourability. A close problem arose in crystallography, of trying to adjust *crystal systems* to *crystal classes* [7].

7.1 Choosing a convenient coordinate system

Although any arbitrary coordinate system could be used, a convenient one must lead to a simple labelling of vertices, so that lattice points have integer indices and indices of symmetric points must moreover display a symmetric pattern. The previous section revealed two kinds of possible arrangements, namely "orthogonal" and "hexagonal". Regarding the regular tessellations, this fact is due to the mutual duality between $\{3,6\}$ and $\{6,3\}$ and the self-duality of $\{4,4\}$, and that semiregular grids carry similar symmetries. More thoroughly, if we focus back on the three regular tessellations in Section 2, a *3*-gon, a *4*-gon and a *6*-gon, all regular, act as Voronoi cells in their corresponding dual grid. The symmetry group of a regular n-gon $\{n\}$ is the *dihedral group* D_n of order $2n$. The $2n$ isometries which maps the n-gon onto itself are the n rotations through angles π/n about its center (referred as a center of n-fold rotational symmetry) and the n reflections in its axes as shown in Figure 7.1.1 [1]. Note that D_3 is a subgroup of D_6.

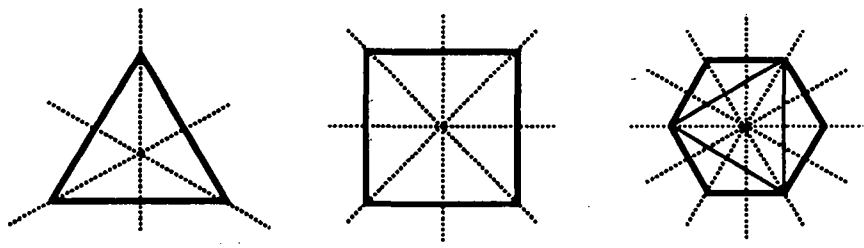

Figure 7.1.1 : The dihedral groups D_3, D_4, D_6

Furthermore we must be aware that the symmetry group $S(T)$ of a tile T in any tiling τ is not necessarily the symmetry group of τ. The group $S(\tau|T)$ of symmetries of T which are also symmetries of τ is called the *stabilizer* of T in τ [4]. A convenient coordinate system should also respect the symmetries of the stabilizer. Note however that in our case : $S(\tau|T) = S({}^{(n)}G|\{n\}) = S(\{n\}) = D_n$.

Figure 7.1.2 : Cartesian and hexagonal systems

Those considerations lead us finally to the choice displayed in Figure 7.1.2. The Cartesian system is the usual one for any orthogonal configuration ; the 2-fold standard basis $B = \{ e_1, e_2 \}$ is induced by the primitive cell (the basic fundamental region). In the hexagonal case, a 2-fold basis $\{ \varepsilon_1, \varepsilon_2 \}$ induced by a primitive cell is obviously sufficient to fix a point ; but if the third axis is somehow superimposed, then the three indices will display a "isotropic" relationship ; so we shall prefer a 3-fold system of generators $S = \{ \varepsilon_1, \varepsilon_2, \varepsilon_3 \}$ instead of a 2-fold basis.

The choice of convenient coordinate systems depending on *crystal classes* is a well-known, important matter in 2D (and 3D) crystallography, so that systems are registered within a nomenclature as *crystal systems* [7]. A similar attention should also be notified in various fields and in networks in particular, regarding the Steiner tree problem [24] wherein hexagonal coordinate systems are sometimes preferred [25].

7.2 Cartesian system

The orthogonal lattice $V = \{(i_1, i_2) \in \mathbf{Z} \times \mathbf{Z} \}$ (or $\mathbf{Z}$ shortly $V = \mathbf{Z}^2$) is spanned by the 2-fold standard basis $B = \{ e_1, e_2 \} = \{ (1,0), (0,1) \}$ of the Cartesian system of Figure 7.1.2, as shown in Figure 7.2.1. The bar over an integer gives a short, neat notation (of crystallographers) to indicate that it is negative.

$\bar{2}2$	$\bar{1}2$	02	12	22
$\bar{2}1$	$\bar{1}1$	01	11	21
$\bar{2}0$	$\bar{1}0$	00	10	20
$\bar{2}\bar{1}$	$\bar{1}\bar{1}$	$0\bar{1}$	$1\bar{1}$	$2\bar{1}$
$\bar{2}\bar{2}$	$\bar{1}\bar{2}$	$0\bar{2}$	$1\bar{2}$	$2\bar{2}$

Figure 7.2.1 : Labelling the orthogonal lattice in Cartesian coordinates

It should be emphasized that the labelling does not depend on the *type* of the grid which will be embedded onto the lattice but only on the *orthogonal* arrangement of the lattice. Referring to the various types of Section 6.1, depending on whether the grid is of type ${}^4G$, ${}^6G$, ${}^3G$, ${}^{(3,6)}G$ or ${}^{(4,4)}G$, the set of vertices and the set of edges are defined *afterwards*. For example the usual grid ${}^4G$ is defined as follows : ${}^4V = V$ and any vertex (i_1, i_2) is connected to four *neighbours* defined as $(i_1 \pm 1, i_2)$ and $(i_1, i_2 \pm 1)$. A hexavalent grid ${}^6G$ can be defined by : ${}^6V = V$ and any vertex (i_1, i_2) is connected to six neighbours defined as $(i_1 \pm 1, i_2)$, $(i_1, i_2 \pm 1)$, $(i_1 + 1, i_2 + 1)$, $(i_1 - 1, i_2 - 1)$. The trivalent grid ${}^3G$ in Figure 6.1.2(a) can be defined by : ${}^3V = V$ and any vertex (i_1, i_2) such that $(i_1 \equiv i_2 \pmod 2)$ is connected to three neighbours defined as $(i_1 \pm 1, i_2)$ and $(i_1, i_2 - 1)$; but a trivalent grid ${}^3G_k$ can be differently defined as a subgrid of ${}^6G$ induced by the removal of a subset V_k of V (Fig. 6.1.2(b)) by ${}^3V_k = V - V_k$ where $V_k = \{ (i_1, i_2) \in V : i_1 + i_2 \equiv k \pmod 3 \}$ and one definition of ${}^3E_k$ would be : any vertex (i_1, i_2) of the subset $V_{k+1 \pmod 3}$ is connected with three neighbours $(i_1 - 1, i_2)$, $(i_1, i_2 - 1)$ and $(i_1 + 1, i_2 + 1)$. The other configurations of Section 6.1 are let to the reader as an exercise.

On the other hand, it is often useful to adopt a *chromatic* representation of the configuration. Conversely, the coloring has a *combinatorial* nature depending on the type of the grid and in no way on the orthogonal arrangement of the lattice. A good coloring is then defined by a relationship between indices. A 4-valent grid is 2-chromatic, so the set V of vertices of the above defined ${}^4G$ grid can be partitioned into two subsets V_0 and V_1 such that $V_k = \{ (i_1, i_2) \in V : i_1 + i_2 \equiv k \pmod 2 \}$ to yield a bipartite graph. A 6-valent grid is 3-chromatic, so the set V of vertices of the above ${}^6G$ grid can be partitioned into three subsets V_0, V_1, V_2 such that $V_k = \{ (i_1, i_2) \in V : i_1 + i_2 \equiv k \pmod 3 \}$. A 3-valent grid is 2-chromatic and the set V of vertices of the above ${}^3G$ grid of Fig. 6.1.2(a) admit the same colouring as in ${}^4G$ since ${}^3G$ can be defined from ${}^4G$ by the removal of any edge $((i_1, i_2), (i_1, i_2 + 1))$ where $(i_1 \equiv i_2 \pmod 2)$ and since this removal preserves the colouring of ${}^4G$; but besides, concerning the 3-valent grid ${}^3G_k$ in Fig. 6.1.2(b) a good 2-colouring is readily induced by the 3-colouring in ${}^6G$ since for instance in ${}^3G_0$ we have : ${}^3V_0 = V - V_0 = V_1 \cup V_2$. Finally the configurations ${}^{(6,3)}G$ and ${}^{(4,4)}G$ (Fig. 6.1.3-4) are readily 2-coloured by the bipartition of the set of vertices into both species, that is, switches and processing nodes.

7.3 *Hexagonal system*

A hexagonal system is set up as follows (Figure 7.3.1). Let $O a_1 a_2 a_3$ be a system of three axes $2\pi/3$ apart going through the origin and denoted counterclockwise. Let M be any point in the plane and α_1, α_2, α_3 the three lines through M parallel to the respective axes ; α_1 meets a_2 and a_3 in M_2 and M'_3 ; α_2 meets a_3 and a_1 in M_3 and M'_1 ; α_3 meets a_1 and a_2 in M_1 and M'_2. Let h_k (resp. h'_k) be the abscissae of any M_k (resp. M'_k). The triplet (h_1, h_2, h_3) (resp. (h'_1, h'_2, h'_3)), relative to M, defines such a hexagonal coordinate system ("HCS"). Note that there exist other ways of setting an *HCS*, for example reversing one axis would define another consistent *HCS*. Nevertheless, our "isotropic" choice yields only both cases hereto.

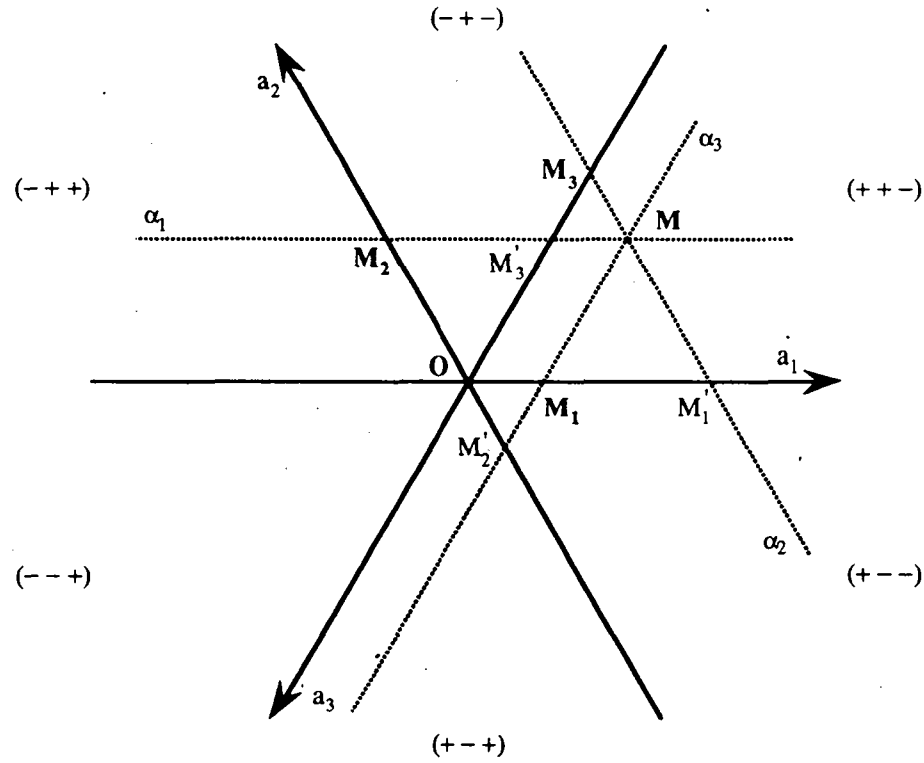

Figure 7.3.1 : Hexagonal coordinate systems

Lemma 7.3.1 For any point of the plane : $(h'_1, h'_2, h'_3) = (-h_3, -h_1, -h_2)$.

Proof Observing the equilateral triangle OM'_1M_3, we have : $|h'_1| = -h_3$.
Now, in each sextant is displayed a symbol giving the sign of coordinates for any point inside it. Thus in particular, in the sextants $(+ + -)$, $(- - +)$ relevant to M'_1M_3, h'_1 and h_3 have opposite signs. Hence $h'_1 = -h_3$.
Two similar argumentations complete the proof •

In the following we shall henceforth consider the *HCS* related to the $\{M_k\}$, unless mentioned otherwise.

Theorem 7.3.1 The coordinates (h_1, h_2, h_3) of any M satisfy the dependence relationship :

$$h_1 + h_2 + h_3 = 0.$$

Proof Focusing first on case M is lying in sextants $(+ + -)$ or $(- - +)$ we must show that : $|h_1| + |h_2| = |h_3|$. Equality of relevant equilateral triangles yields :

$$|h_3| = OM_3 = OM'_3 + M'_3M_3 = OM_2 + OM_1 = |h_2| + |h_1|.$$

Two similar argumentations complete the proof •

Definition 7.3.1 The set $S=\{\varepsilon_1,\varepsilon_2,\varepsilon_3\}=\{(1,0,-1),(-1,1,0),(0,-1,1)\}$ defines an ordered system of generators for the HCS. Furthermore, the hexagonal lattice is defined as :

$$V=\{(h_1,h_2,h_3)\in Z^3 \ : \ h_1+h_2+h_3=0\}$$

and spanned by S.

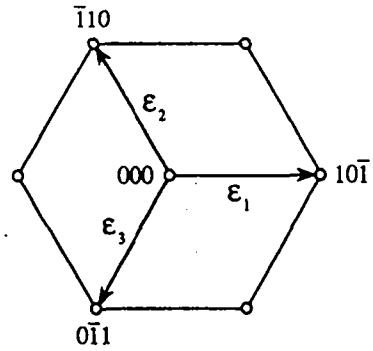

Figure 7.3.2 : A system of generators for the HCS

The generators ε_1, ε_2, ε_3 of S are defined as in Figure 7.3.2 from the construction of the HCS, that is, with the point M respectively on α_1, α_2, α_3 axis and, on the other hand, in order that a primitive cell have a unit area. The lattice is labelled accordingly, as shown in Figure 7.3.3. Those indices are closely related to the Bravais-Miller indices in crystallography [7].

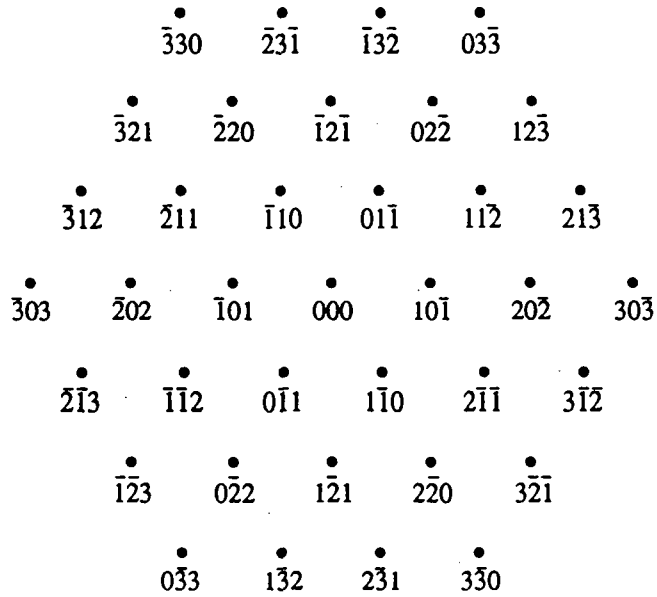

Figure 7.3.3 : Labelling the lattice in hexagonal coordinates

Proposition 7.3.1 For any vertex (h_1,h_2,h_3) of V : $h_1 - h_2 \equiv h_2 - h_3 \equiv h_3 - h_1 \pmod 3$.

Proof The relation holds at the origin then we prove that by induction. Any vertex (h_1, h_2, h_3) is surrounded by six vertices (h'_1, h'_2, h'_3) with $h'_k = h_k + \delta_k$, where $\delta_k \in \{-1, 0, 1\}$ provided that $\sum \delta_k = 0$. This implies : $\delta_1 - \delta_2 \equiv \delta_2 - \delta_3 \equiv \delta_3 - \delta_1 \pmod 3$. Hence the relation holds for any (h'_1, h'_2, h'_3) •

The proposition allows to partition V into three subsets V_k $(k=0,1,2)$ where $V_k = \{(h_1,h_2,h_3) \in \mathbf{Z}^3 : h_1 - h_2 \equiv k \pmod 3\}$. Moreover, this partitioning yields a good 3-coloring of V within the 6-valent grid (for general results on color groups, the reader is referred to Senechal [26]).

As for the CCS, once the HCS is set up, the different types of grids can be defined afterwards. Compare the definitions below with their (isomorphic) grids in Section 7.2. The hexavalent grid ${}^6G$ is defined as follows : ${}^6V = V$ and any vertex (h_1,h_2,h_3) is connected to six *neighbours* $(h_1+\delta_1,\ h_2+\delta_2,\ h_3+\delta_3)$ where the δ_k are as above. Any trivalent grid ${}^3G_k$ of Figure 6.2.3 can be defined in a concise way by : ${}^3V_k = V - V_k$ and any vertex $\boldsymbol{h}$ of $V_{k+1 \pmod 3}$ is connected to three neighbours $\boldsymbol{h}+\varepsilon_1$, $\boldsymbol{h}+\varepsilon_2$, $\boldsymbol{h}+\varepsilon_3$. Any semiregular grid ${}^{(3,6)}G_k$ of Figure 6.2.4 is simply defined by ${}^{(3,6)}V_k = V$ and any vertex of V_k is connected to the six corresponding neighbours of the above ${}^6G$.

Of course, the triplet of 4-valent grids ${}^4G_k$ $(k=1,2,3)$ embedded in ${}^6G$ according to Figure 6.2.1 can be defined in this way. But it is more interesting to show that a 2-fold basis G_k can be assigned to ${}^4G_k$ following a straightforward rule in the HCS. Consider such a 4-valent grid ${}^4G_1$ defined as a spanning subgrid of ${}^6G$ by removing one direction of edges, say the direction of a_1 axis.

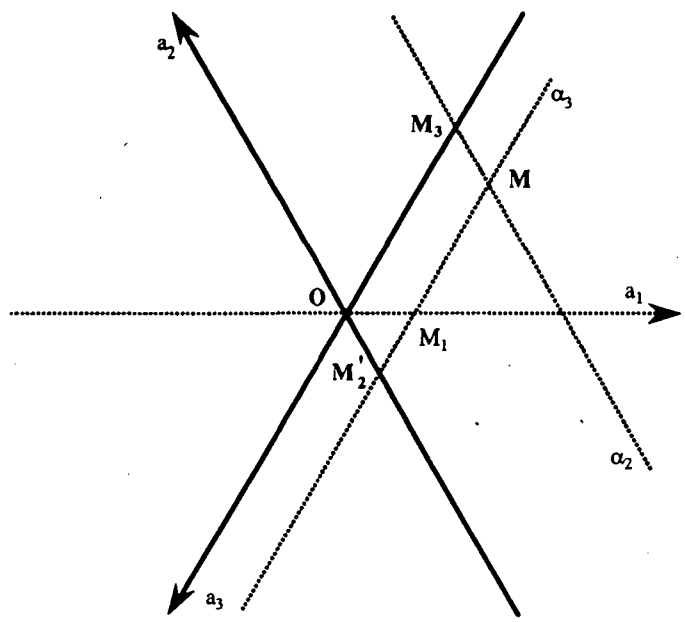

Figure 7.3.4 : A 2-fold system assigned to a 4-valent grid

Let us refer to the HCS in Figure 7.3.1 and remove the corresponding axis (included the parallel line α_1). Then α_2 meets a_3 in M_3 and α_3 meets a_2 in M'_2. Unfortunately, M'_2 does not belong to our standard HCS. However, its abscissa satisfies $h'_2 = -h_1$ from Lemma 7.3.1 and as shown in Figure 7.3.4. Hence, from the system of generators S, we can extract a 2-fold basis B_1. Any point M with coordinates (h_1, h_2, h_3) in S is now defined by $(-h_1, ., h_3)$ in the new basis $B_1 = \{(-1, ., 0), (0, ., 1)\}$, the dot meaning that the irrelevant indice is omitted. Thus it is now easy to define a 4-valent grid exactly as it was done in the CCS. Here for ${}^4G_1$ we have : ${}^4V_1 = V$ and any vertex $(h_1, ., h_3)$ is connected to four *neighbours* $(h_1 \pm 1, ., h_3)$ and $(h_1, ., h_3 \pm 1)$.

In a similar way, removing a_2 axis yields $M \to (h_1, -h_2, .)$ in $B_2 = \{(0, ., -1), (1, ., 0)\}$ and removing a_3 axis yields $M \to (., h_2, -h_3)$ in $B_3 = \{(., 0, -1), (., 1, 0)\}$, M lying in the whole plane.

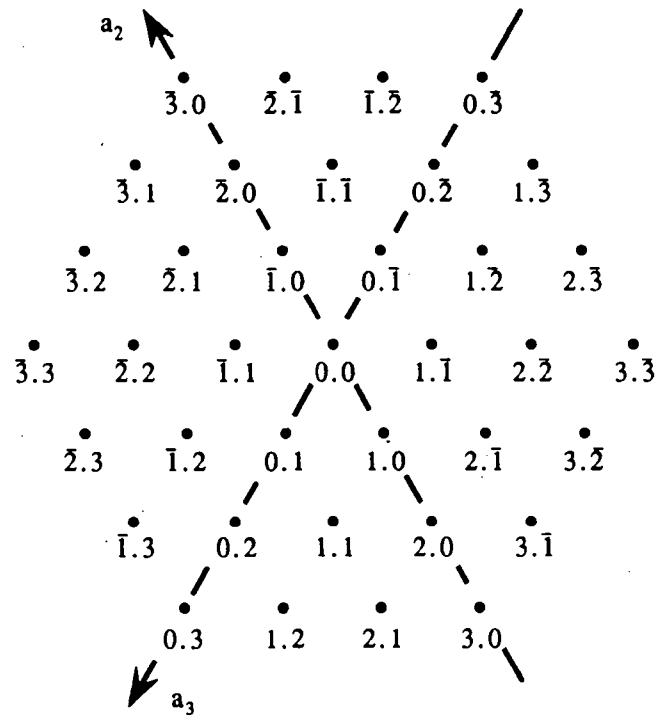

Figure 7.3.5 : Two-fold labelling in the HCS

7.4 Correspondance between Cartesian and hexagonal systems

In spatial applications a point is usually expressed by its coordinates in the Cartesian system. However, the 2D scene may be partitioned into *hexagonal* cells whose control is assigned to a network of processing nodes, following a divide-and-conquer allocation strategy. In this case the HCS fits well the hexagonal tessellation. But a correspondence between both systems should be somehow set up. Let Oxy be the CCS with Ox on Oa_1. Let $M \to \boldsymbol{h} = (h_1, h_2, h_3)$ in the HCS as above and $M \to \boldsymbol{u} = (x, y)$ in the CCS as shown in Figure 7.4.1.

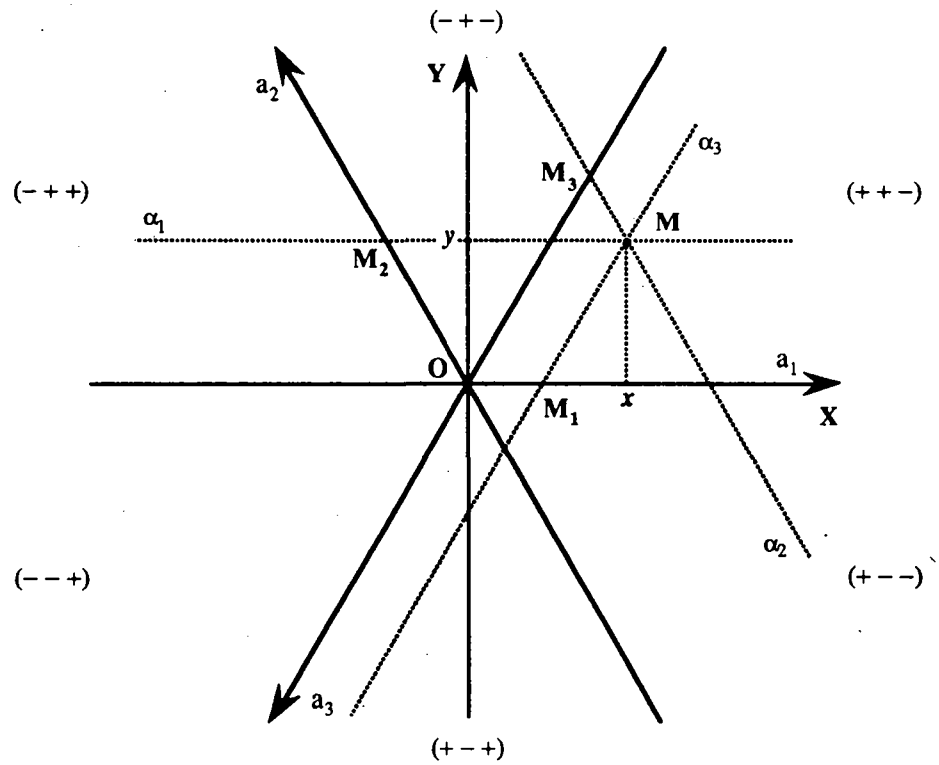

Figure 7.4.1 : Cartesian and hexagonal systems

Lemma 7.4.1 The correspondence between coordinates of any M in HCS and CCS is given by : $\boldsymbol{h} = \boldsymbol{A}\ \boldsymbol{u}$ where :

$$\boldsymbol{A} = \begin{bmatrix} 1 & \frac{-1}{\sqrt{3}} \\ 0 & \frac{2}{\sqrt{3}} \\ -1 & \frac{-1}{\sqrt{3}} \end{bmatrix}$$

Proof Immediate •

Often it will be interesting to settle the correspondence with only a 2-fold subset of $\boldsymbol{h}$. A typical example is illustrated by the previous decomposition of ${}^6G$ into three 4-valent grids.

Corollary 7.4.1 For any subset $\boldsymbol{h}_{rs} = (h_r, h_s)$ of $\boldsymbol{h}$, the inverse correspondence between CCS and HCS is given by $\boldsymbol{u} = \boldsymbol{A}_{rs}\,\boldsymbol{h}_{rs}$ where :

$$\boldsymbol{A}_{12} = \begin{bmatrix} 1 & \frac{1}{2} \\ 0 & \frac{\sqrt{3}}{2} \end{bmatrix} \qquad \boldsymbol{A}_{23} = \begin{bmatrix} -\frac{1}{2} & -1 \\ \frac{\sqrt{3}}{2} & 0 \end{bmatrix} \qquad \boldsymbol{A}_{31} = \begin{bmatrix} \frac{-\sqrt{3}}{2} & \frac{-\sqrt{3}}{2} \\ \frac{1}{2} & \frac{-1}{2} \end{bmatrix}$$

•

8 Conclusion

The purpose of this paper was to reduce the apparent disorder prevailing in the world of grids and, consequently, to help future developments in the topic of massively parallel architectures. A huge material required as a background was borrowed from manifolds fields, so the content of their contributive part has just been outlined in our concern. In particular, just a little bit of tiling and pattern theory was used ; rich results of regular graphs did not serve once ; a thorough inventory of the seventeen wallpaper groups in crystallography was discarded ; while a lack of use of Cayley's representation, yet acknowledged as a useful tool for analysis in discrete groups, can be notified. Hence this attempted terminology suffers somewhat from weakness and much would remain to be done. But our proposal was first and foremost enumerative, so we merely hope it may serve as an introductive startpoint for further developments in the topic.

References

[1] H. S. M. Coxeter : *Introduction to Geometry.*
Wiley, New York (1961). Second ed. (1969).

[2] L. Fejes Toth : *Regular Figures.*
Pergamon, New York (1964).

[3] H. S. M. Coxeter, W. O. J. Moser : *Generators and Relations for Discrete Groups.*
Springer, Berlin (1957). Fourth ed. (1980).

[4] B. Grünbaum, G. C. Shephard : *Tilings and Patterns.*
Freeman & Co., New York (1987).

[5] F. Harary : *Graph Theory.*
Addison-Wesley, Reading Massachusets (1969).

[6] N. Biggs : *Algebraic Graph Theory.*
Cambridge Univ. Press, London (1974).

[7] M. J. Buerger : *Introduction to Crystal Geometry.*
McGraw-Hill, New York (1971).

[8] S.H. Unger : A computer oriented toward spatial problems.
Proc. IRE, 46 (1958) 1744-50.

[9] R. Sibson : The Dirichlet tessellation as an aid in data analysis.
Scandinavian Journal of Statistics, 7 (1980) 14-20.

[10] A. Rosenfeld : Adjacency in digital pictures.
Information and Control 26 (1974) 24-33.

[11] L. Snyder : Introduction to the configurable, highly parallel computer.
Computer 15 (1) (1982) 47-56.

[12] G.H. Barnes *et al.* : The ILLIAC IV Computer.
IEEE Trans. Comp. C-17 (8) (1968) 746-757.

[13] J. Rattner : The new age of supercomputing. *Distributed Memory Computing, Lecture Notes in Computer Science* 487, A. Bode ed., Springer-Verlag (1991) 1-6.

[14] H.T. Kung, C. Leiserson : Algorithms for VLSI processor arrays In *C. Mead & L. Conway, Introduction to VLSI Systems*, Addison-Wesley (1980).

[15] P. Quinton, Y. Robert : *Algorithmes et architectures systoliques*. Masson (1989). English version : *Systolic algorithms and architectures*. Prentice-Hall (1991).

[16] A.L. Liestman, T.S. Shermer : Grid and hypercube spanners. *CMPT TR 91-1* Simon Fraser University, Burnaby, Canada (1991).

[17] D. Peleg, A.A. Schäffer : Graph spanners. *Journal of Graph Theory* 13 (1989) 99-116.

[18] D. Blewins, E. Davis, R. Heaton, J. Reif : BLITZEN: A highly integrated massively parallel machine. *Journal of Par. and Dist. Comp.*, 8 (2) (1990) 150-60.

[19] T. Blank : The MasPar MP-1 architecture. *Proc. IEEE Compcon Spring*, IEEE (1990) 20-24.

[20] B.H. McCormick : The Illinois pattern recognition computer - ILLIAC III. *IEEE Trans. Elec. Comp.*, EC-12 (1963) 791-813.

[21] M.J.E. Golay : Hexagonal parallel pattern transformations. *IEEE Trans. Comp.*, C-18 (8) (1969) 733-740.

[22] A.L. Davis, S.V. Robison : The architecture of the FAIM-1 symbolic multiprocessing system. *Proc. 9th Int. Joint. Conf. on Artificial Intelligence* (1985) 32-38.

[23] M.S. Chen, K.G. Shin, D.D. Kandlur : Addressing, routing, and broadcasting in hexagonal mesh multiprocessors. *IEEE Trans. Comp.* 39 (1) (1990) 10-18.

[24] F.K. Hwang, D.S. Richards, P. Winter : The Steiner tree problem. *Annals of Discrete Math.* 53, North Holland (1992).

[25] F.K. Hwang, J.F. Weng : Hexagonal coordinate systems and Steiner minimal trees. *Discrete Math.* 62 (1986) 49-57.

[26] M. Senechal : Color groups. *Discrete Applied Math.* 1 (1979) 51-73.

Unité de recherche INRIA Rennes
IRISA, Campus universitaire de Beaulieu 35042 Rennes Cedex (France)
Unité de recherche INRIA Lorraine - Technopôle de Nancy-Brabois - Campus scientifique
615, rue du Jardin Botanique - B.P. 101 - 54602 Villers lès Nancy Cedex (France)
Unité de recherche INRIA Rhône-Alpes - 46, avenue Félix Viallet - 38031 Grenoble Cedex 1 (France)
Unité de recherche INRIA Rocquencourt - Domaine de Voluceau - Rocquencourt - B.P. 105 - 78153 Le Chesnay Cedex (France)
Unité de recherche INRIA Sophia Antipolis - 2004, route des Lucioles - B.P. 93 - 06902 Sophia Antipolis Cedex (France)

Éditeur
INRIA - Domaine de Voluceau - Rocquencourt - B.P. 105 - 78153 Le Chesnay Cedex (France)

ISSN 0249 - 6399